MOLECULAR AND CELLULAR BIOLOGY, Apr. 2008, p. 2637–2647 Vol. 28, No. 8
0270-7306/08/$08.00+0 doi:10.1128/MCB.01601-07

Mice Lacking Homer 1 Exhibit a Skeletal Myopathy Characterized by Abnormal Transient Receptor Potential Channel Activity▽†

Jonathan A. Stiber,[1] Zhu-Shan Zhang,[1] Jarrett Burch,[1] Jerry P. Eu,[1] Sarah Zhang,[2] George A. Truskey,[2] Malini Seth,[1] Naohiro Yamaguchi,[3] Gerhard Meissner,[3] Ripal Shah,[1] Paul F. Worley,[4] R. Sanders Williams,[1] and Paul B. Rosenberg[1]*

Department of Medicine, Duke University Medical Center, Durham, North Carolina 27710[1]; Department of Biomedical Engineering, Duke University, Durham, North Carolina 27710[2]; Department of Biochemistry and Biophysics, University of North Carolina at Chapel Hill, Chapel Hill, North Carolina 27599[3]; and Department of Neuroscience, Johns Hopkins University, Baltimore, Maryland 21205[4]

Received 30 August 2007/Returned for modification 1 October 2007/Accepted 19 January 2008

Transient receptor potential (TRP) channels are nonselective cation channels, several of which are expressed in striated muscle. Because the scaffolding protein Homer 1 has been implicated in TRP channel regulation, we hypothesized that Homer proteins play a significant role in skeletal muscle function. Mice lacking Homer 1 exhibited a myopathy characterized by decreased muscle fiber cross-sectional area and decreased skeletal muscle force generation. Homer 1 knockout myotubes displayed increased basal current density and spontaneous cation influx. This spontaneous cation influx in Homer 1 knockout myotubes was blocked by reexpression of Homer 1b, but not Homer 1a, and by gene silencing of TRPC1. Moreover, diminished Homer 1 expression in mouse models of Duchenne's muscular dystrophy suggests that loss of Homer 1 scaffolding of TRP channels may contribute to the increased stretch-activated channel activity observed in *mdx* myofibers. These findings provide direct evidence that Homer 1 functions as an important scaffold for TRP channels and regulates mechanotransduction in skeletal muscle.

Mechanosensitive ion channels through their interactions with cytoskeletal proteins link mechanical stimuli such as stretch and changes in osmolarity with signaling pathways. In this way, stretch-activated channel activity is governed by the mechanical properties of the plasma membrane that are established by the underlying cytoskeleton (8). As mechanical forces reach the cytoskeleton, channel activity is increased, setting in motion a series of biochemical events that provide an adaptive response to mechanical stimulation. Increased transient receptor potential (TRP) channel activity has long been associated with pathological features of muscle dystrophy, where a mutation in a dystrophin results in altered membrane integrity and increased stretch-activated channel activity (16, 37).

Homer proteins are a family of multifaceted scaffolding proteins that enhance signaling efficiency by linking transmembrane proteins with signaling complexes. For example, Homer proteins bind to metabotropic glutamate receptors, clustering them to the postsynaptic density and modulating the excitatory actions of glutamate (1, 34). All Homer proteins share a highly conserved Ena/vasodilator-stimulated phosphoprotein homology 1 (EVH1) domain at their amino termini that allows binding to proline-rich motifs on Homer ligands, which include metabotropic glutamate receptors, inositol 1,4,5-triphosphate receptors (IP3Rs), and several members of the TRP channel family (23, 35, 43). Constitutively expressed Homer isoforms such as Homer 1b and 1c, in addition to containing an amino-terminal EVH1 domain, also contain a C-terminal coiled-coil domain, allowing Homer proteins to self-multimerize (15). Homer 1a, which was identified as an immediate-early gene, lacks a C-terminal coiled-coil domain and is postulated to function as a dominant negative isoform (10). The different isoforms of Homer genes including the immediate-early gene isoforms are the result of alternative splicing (5).

Recent work has shown that Homer 1 interacts with several members of the TRPC family of TRP channels and mediates the formation of a large macromolecular complex involving IP3R and TRPC channels (43). Mutations of the Homer binding site of TRPC1 or coexpression of Homer 1a and TRPC1 in cells results in increased TRPC1 channel activity. Pancreatic acinar cells lacking Homer 1 exhibit abnormal calcium entry, with a 2.5-fold increase in spontaneous calcium influx compared to cells from wild-type mice (43). In addition, a mutation in the *Drosophila* Homer locus leads to abnormal motor activity and coordination (7).

Homer proteins are expressed in skeletal muscle and localize to the Z-disk/costamere complex (26). Homer protein expression is highly regulated in skeletal muscle, as indicated by expression profiling studies using models of muscle regeneration and mechanical overload (4, 28). As to the function of Homer in muscle, several studies have focused on the interaction of Homer with either the IP3R or ryanodine receptor in skeletal muscle (26, 38). Recently, our group observed that Homer is expressed as part of the myogenic differentiation program, the function of which is to enhance muscle differentiation through modulation of calcium-dependent gene expression (31). Homer enhances calcium signaling via the calcineurin/NFAT (nuclear factor of activated T cells) pathway,

* Corresponding author. Mailing address: Department of Medicine, Duke University Medical Center, 4321 Medical Park Drive, Suite 200, Durham, NC 27704. Phone: (919) 479-2315. Fax: (919) 477-0632. E-mail: rosen029@mc.duke.edu.

† Supplemental material for this article may be found at http://mcb.asm.org/.

▽ Published ahead of print on 11 February 2008.

resulting in greater activation of a muscle-specific transcriptional program.

To determine the function of Homer in adult muscle, we examined the histological and functional properties of skeletal muscle from Homer 1 knockout (KO) mice. The generation of Homer 1 KO mice has been described by Yuan et al. (43). These mice have previously been shown to display complex behavioral abnormalities and impaired urinary bladder function (18, 32). Here, we show that mice lacking Homer 1 exhibit a myopathy characterized by decreased fiber cross-sectional area and skeletal muscle force generation. Loss of Homer 1 in primary myotubes resulted in increased basal current density, increased basal cytosolic [Ca^{+2}], and spontaneous cation influx consistent with abnormal TRP channel activation. This spontaneous cation influx in Homer 1 KO myotubes was blocked by reexpression of the coiled-coil Homer isoform, Homer 1b, and by gene silencing of TRPC1. Skeletal muscle from Homer 1 KO mice shows upregulation of calpastatin and sarcoplasmic reticulum $Ca2^{+}$ ATPase 1 (SERCA1) protein expression, indicating that excessive calcium influx contributes to the myopathy of these mice.

MATERIALS AND METHODS

Measurement of skeletal muscle contractility. Measurement of the contractility of extensor digitorum longus (EDL) muscles from Homer 1 KO mice and wild-type (WT) littermates was performed using an established protocol (9). Homer 1 KO and control mice were anesthetized and euthanized, after which intact EDL muscles were removed and placed in Kreb's buffer (pH 7.4). The intact whole muscles were placed in a 30-ml chamber between platinum stimulating electrodes and bathed in Kreb's buffer, which was continuously aerated with 95% O_2. The muscles were then attached to an isometric force transducer and stretched to a length that produced the maximum tetanic force with field stimulation. The force transducer measurements were recorded and analyzed on a computer using Polyview software (Astro-Med, West Warwick, RI). Muscles were subjected to multiple frequencies of stimulation of 500-ms duration between 1 and 140 Hz to produce the force-frequency relationship and determine the maximal tetanic force. Unless otherwise specified, forces shown are normalized to the muscle cross-sectional area (N/cm^2).

Primary culture of Homer 1 KO and WT myotubes. Skeletal muscle was obtained from the hind limbs of euthanized neonates derived from the mating of breeding pairs heterozygous for loss of the Homer 1 allele. Tail clips were obtained simultaneously for genotyping of Homer 1 +/+, +/−, and −/− neonates obtained from these matings. Skeletal muscle from neonates was digested in trypsin for 30 min, followed by the addition of soybean trypsin inhibitor and type VII collagenase (Sigma) for an additional 30 min. Digested muscles were pelleted by centrifugation, resuspended, and preplated on plastic culture plates for 2 h for removal of fibroblasts. Cells were then plated on fibronectin (Roche)-coated tissue culture plates. After proliferation in Dulbecco's modified Eagle's medium containing 20% fetal bovine serum, myoblasts were then allowed to differentiate into myotubes in low-serum medium (Dulbecco's modified Eagle's medium with 2% horse serum). Unless otherwise specified, measurements of calcium transients and transverse mechanical properties were performed on day 5 myotubes, i.e., myotubes that were allowed to differentiate for 5 days in low-serum medium.

AFM. The transverse mechanical properties of primary myotubes were measured using a Bioscope atomic force microscopy (AFM) probe mounted on an inverted microscope as described previously (6). AFM uses a cantilever arm that comes in contact with the cell to induce cellular deformations. The force applied was calculated from Hooke's law and is the product of the spring constant, k, and the deflection of the cantilever, d. The equal and opposing force with which the myotube resists was estimated by using the Hertz model. From this known force, the apparent elastic modulus can be calculated. Myotube stiffness is inversely proportional to the amount of deformation as expected from the spring equation (Hooke's law): that is, for a given force applied to the myotube surface, the greater the resultant deformation, the less stiff the myotube and the lower the transverse apparent elastic modulus. The elastic properties are defined as an apparent elastic modulus because there are viscous contributions within the cellular response and nonlinear elastic behavior that is not apparent from the deformations studied (6).

Calcium imaging. Primary myoblasts were grown and allowed to differentiate into myotubes on glass-bottom plates (Mattek) and subsequently loaded with 10 μM fura 2-AM (fura-2-acetoxymethyl ester; Molecular Probes, Eugene, OR) for 30 min for measurements of calcium transients in response to agonists. Fura-2-AM-loaded cells were illuminated by alternating 340/380-nm light delivered every 300 ms by a DG-4 argon exciter (Sutter Instruments, Novato, CA) under the control of MetaFluor software, and fluorescence images were captured at an emission of 510 nm with a Photometrics Cool SNAP HQ charge-coupled device camera (Roper Scientific, Tucson, AZ) based on a Nikon TE2000 fluorescent microscope. Measurements of cytosolic calcium concentration were performed using the method described by Grynkiewicz et. al (12).

Whole-cell patch clamp recordings. Patch clamp experiments were performed to record currents in the whole-cell mode with pipettes filled with a low-chloride pipette solution containing 120 mM cesium aspartate, 10 mM CsCl, 1 mM $MgCl_2$, 10 mM HEPES, 5 mM EGTA, pH 7.2 (with CsOH), and 295 mosM (with D-mannitol). The extracellular bath included a low-chloride and potassium solution containing 130 mM sodium aspartate, 6 mM NaCl, 2 mM $CaCl_2$, 1 mM $MgCl_2$, 10 mM HEPES, 10 mM glucose, pH 7.4 (with NaOH), and 305 mosM (with D-mannitol). Potassium channel activity was blocked by replacing potassium with cesium in the solutions. L-type Ca^{2+} channel activity was blocked by 10 μM verapamil in external solution. The voltage-dependent sodium channel was inactivated by the stimulation protocol, and chloride current was inhibited by a reduced and equal chloride ion concentration in the external and internal solution, or 1 mM anthracene-9-carboxylic acid in the external solution. The osmolarity of each solution was verified with a freezing-point osmometer (Advanced Instruments). Voltage across the cell-attached membrane patch was controlled, and currents were recorded using an Axonpatch-200A amplifier with Digidata 1200 interface and analyzed with pCLAMP software. Currents were induced by 200-ms voltage ramp protocols (1 mV/ms, from 100 mV to −100 mV), at a holding potential of −60 mV. Experiments were performed at room temperature with a sample rate of 4 kHz (filter, 2 kHz). GsMTx4, a spider venom peptide, was used in certain experiments as an inhibitor of mechanosensitive channels (Peptides International, Louisville, KY).

Western blotting, coimmunoprecipitation, immunohistochemistry, and reverse transcription-PCR (RT-PCR). Dissected muscles from euthanized mice were homogenized using a glass mortar and pestle in either 1% Triton lysis buffer containing 1% Triton X-100, 150 mM NaCl, 50 mM Tris, pH 8, and protease inhibitor (Complete Mini; Roche, Mannheim, Germany) or lysis buffer containing 50 mM Tris, pH 7.6, 500 mM NaCl, 0.1% sodium dodecyl sulfate (SDS), 0.5% deoxycholate, 1% Triton X-100, and protease inhibitor. Protein concentrations were measured by the Bradford assay for equal loading and subsequent analysis by SDS-polyacrylamide gel electrophoresis (PAGE) and Western blotting. Protein transfer was confirmed by Ponceau staining, and equal loading was confirmed by immunoblotting for α-tubulin (Santa Cruz Biotechnology, Santa Cruz, CA). In coimmunoprecipitation assays, muscles were homogenized in 1% Triton X-100 lysis buffer as above. A rat pan-Homer antibody (Ab) and protein G-Sepharose (Amersham Biosciences, Uppsala, Sweden) were used for immunoprecipitation, followed by SDS-PAGE and immunoblotting for TRPC1. For immunofluorescence studies, muscles were frozen in 22-oxyacalcitriol and then cryo-sectioned. Homer immunoblotting, immunoprecipitation, and immunofluorescence studies were performed using a rat pan-Homer Ab that recognizes all Homer isoforms (Chemicon, Temecula, CA). Rabbit anti-α-actinin Ab used in immunofluorescence studies was obtained from Sigma (St. Louis, MO), and mouse anti-SERCA1 Ab was obtained from Affinity Bioreagents (Golden, CO). TRPC1 Ab was generated with the assistance of Larial Proteomics (Ontario, Canada) using the carboxy-terminal 20 amino acids of TRPC1 (GFRTSKYAM FYPKNC). Validation of this antibody is available at www.larial.com.

Cloning of Homer 1 isoforms and TRPC1 gene silencing. PCR primers were used to amplify the open reading frames of Homer 1a and Homer 1b from adult mouse skeletal muscle as described by Sandona et al. (27). PCR products for Homer 1a and Homer 1b were then subcloned into the PCI-Neo vector (Promega) using the EcoRI restriction site, and the correct orientation was confirmed by sequencing. DNA templates for the synthesis of silencing RNA were cloned into an expression plasmid for subsequent transfection. The selection of the coding sequence for targeting TRPC1 mRNA was done by using the small interfering RNA target finder and design tool from Ambion. The potential target sequence was subjected to a BLAST search against mouse expressed sequence tag libraries to ensure specificity of the target. The oligonucleotide sequences were the following: *SIL A* construct, 5′-GATCCCCCATAAATTGCGTAGATGTGTTCAA GAGACACATCTACGCAATTTATGTTTTTGGAAA-3′ (sense) and 3′-GGGG TATTTAACGCATCTACACAAGTTCTCTGTGTAGATGCGTTAAATACAA

AAACCTTTTCGA-5′ (antisense); *SIL B* construct, 5′-GATCCCCGGGTGACTATTATATGGTTTTCAAGAGAAACCATATAATAGTCACCCTTTTTGGAAA-3′ (sense) and 3′-GGGCCCACTGATAATATACCAAAAGTTCTCTTTGGTATATTATCAGTGGGAAAAACCTTTTCGA-5′ (antisense); *SIL C* construct (noneffective), 5′-GATCCCCAGCAACGACACCTTCCACTTTCAAGAGAAGTGGAAGGTGTCGTTGCTTTTTTGGAAA-3′ (sense) and 3′-GGGTCGTTGCTGTGGAAGGTGAAAGTTCTCTTCACCTTCCACAGCAACGAAAAAACCTTTTCGA-5′ (antisense). Primary myocytes were transfected with empty vector expressing yellow fluorescent protein (YFP) and either TRPC1 silencing plasmids or scrambled control plasmids using Fugene reagent (Roche). YFP-positive cells were studied 5 days posttransfection.

Statistics. Data are presented as means ± standard errors of the means. An unpaired Student's *t* test was used for comparison between two groups, and analysis of variance with Tukey-Kramer's test was used for comparison among groups. Values of P of <0.05 were considered significant.

RESULTS

Spatial distribution of Homer in skeletal muscle. Homer proteins are expressed in a variety of tissues including skeletal muscle, where there is expression of both Homer 1 and Homer 2 isoforms (27, 28). Homer proteins are often localized into specialized regions of a cell, e.g., the postsynaptic density (14, 34). Using immunohistochemical localization of Homer proteins in adult skeletal muscle, we found that Homer localizes in a repetitive band pattern that overlaps with staining for α-actinin, supporting previous observations that Homer localizes to the Z-disk (Fig. 1A to C) (26). The Z-disk forms the lateral boundary of the sarcomere, anchors actin thin filaments, and plays an essential role in the lateral transmission of force generated by actin-myosin cross-bridging (3, 8).

Histologic sections and protein lysates taken from mice lacking Homer 1 demonstrate minimal expression of Homer even with a pan-Homer Ab that recognizes all Homer isoforms, confirming that Homer 1 isoforms are the predominant isoforms in skeletal muscle (Fig. 1E and F). However, a small quantity of Homer protein was detected in the lysates from slow-twitch muscle (soleus) (Fig. 1F). These results are consistent with previous studies that indicate that coiled-coil Homer 1 isoforms are the predominant isoforms in skeletal muscle and that residual Homer expression in slow-twitch muscle represents Homer 2, which we previously have shown is preferentially expressed in slow-twitch muscle (28, 31). RT-PCR was performed using primers and conditions described by Sandona et al. for amplification of coiled-coil Homer 1 isoforms (27). RT-PCR using cDNA prepared from plantaris muscle resulted in amplification of two distinct bands of the predicted size, corresponding to Homer 1b and Homer 1c (Fig. 1G, H1b and H1c, respectively), which differed in size by about 30 bp. The identity of the amplified products was later confirmed by direct sequencing.

Since several muscular dystrophies result from mutations in proteins residing in the Z-disk/costamere, we were interested to understand if muscles from Homer 1 KO mice displayed features of muscle damage consistent with myopathy (2). To determine whether myopathic changes exist in Homer KO mice, we performed immunostaining for dystrophin in frozen sections of skeletal muscle from Homer 1 KO mice and WT littermates at 8 weeks of age. We observed no changes in dystrophin staining, suggesting the preservation of plasma membrane integrity (Fig. 1H). We also saw no significant difference in the frequencies of central nucleation, a marker of myofiber degeneration/regeneration, between Homer 1 KO mice and WT littermates (1.1% ± 0.4% for Homer 1 KO versus 0.6% ± 0.2% for WT mice; data are the mean ± standard error [SE]; $P = 0.26$). However, automated analysis of the fiber cross-sectional area with Metamorph software (Molecular Devices, Sunnyvale, CA) did detect a significant difference in the cross-sectional area of myofibers from muscles of Homer 1 KO mice compared with WT littermates (Fig. 1I). The fiber cross-sectional area was $42.1 \times 10^2 \pm 80\ \mu m^2$ in Homer 1 KO mice versus $53.6 \times 10^2 \pm 65\ \mu m^2$ in WT littermate controls (mean ± SE; $P < 0.05$). The distribution of muscle fiber cross-sectional areas was as shown in Fig. 1J.

Homer 1 KO mice exhibit decreased skeletal muscle contractility. Homer 1 KO mice were previously noted to show complex alterations in learning and behavior as well as an increased predilection to cocaine addiction. Behavioral testing revealed a variety of deficits in motor performance including grip strength, rotorod performance, nest building, and vertical activity (32). Although previous reports implicated loss of Homer in defects in motor control in *Drosophila* and in grip strength in mice, few details were available on how Homer influenced muscle performance (7, 32). Consistent with these reports, forced treadmill testing of Homer 1 KO mice and WT littermates revealed that Homer 1 KO mice exhibited a decrease in maximal running speed compared to WT littermates (data not shown). These results indicate a motor defect, but they cannot be used to distinguish a neuronal defect from an intrinsic muscle defect. To determine whether the altered muscle performance was an intrinsic defect in muscle, we isolated EDL muscle to measure contractile force and force-frequency relationships for Homer 1 KO and WT mice. Homer 1 KO mice displayed a delayed relaxation phase and marked reductions in both twitch and tetanic force production (Fig. 2) ($P < 0.05$). Forces generated over a range of stimulation frequencies (1 to 140 Hz) were significantly reduced in Homer 1 KO muscle compared to WT controls even after normalization to muscle cross-sectional area, indicating a primary defect in contractility. Interestingly, there was no significant difference in the frequency at which maximum force was obtained (i.e., a shift in the relative force-frequency curve, in which force at a given frequency is normalized to maximal force obtained) to suggest a defect in excitation-contraction (EC) coupling in Homer 1 KO mice (Fig. 2B). These results indicate a primary defect in contractility, independent of EC coupling (9).

A potential explanation for the reduction in contractile force is the possibility that loss of Homer 1 results in denervation. Homer proteins localize to the postsynaptic density of neurons and could be theorized to play a role in the formation of the neuromuscular junction and activation of acetylcholine receptor signaling. We addressed this possibility by measuring bungarotoxin staining of the motor endplate of skeletal muscle from Homer 1 KO mice and their WT littermates. We observed no significant difference in the presence or numbers of motor endplates between Homer 1 KO muscle and controls, arguing against a myasthenic phenotype as the cause of the force generation defect (for Homer 1 KO, 31 ± 5 [$n = 8$] versus 25 ± 4 [$n = 7$] endplates/cross section for WT; $P = 0.40$).

Abnormal current density in Homer 1 KO myotubes. We observed no significant difference in resting membrane poten-

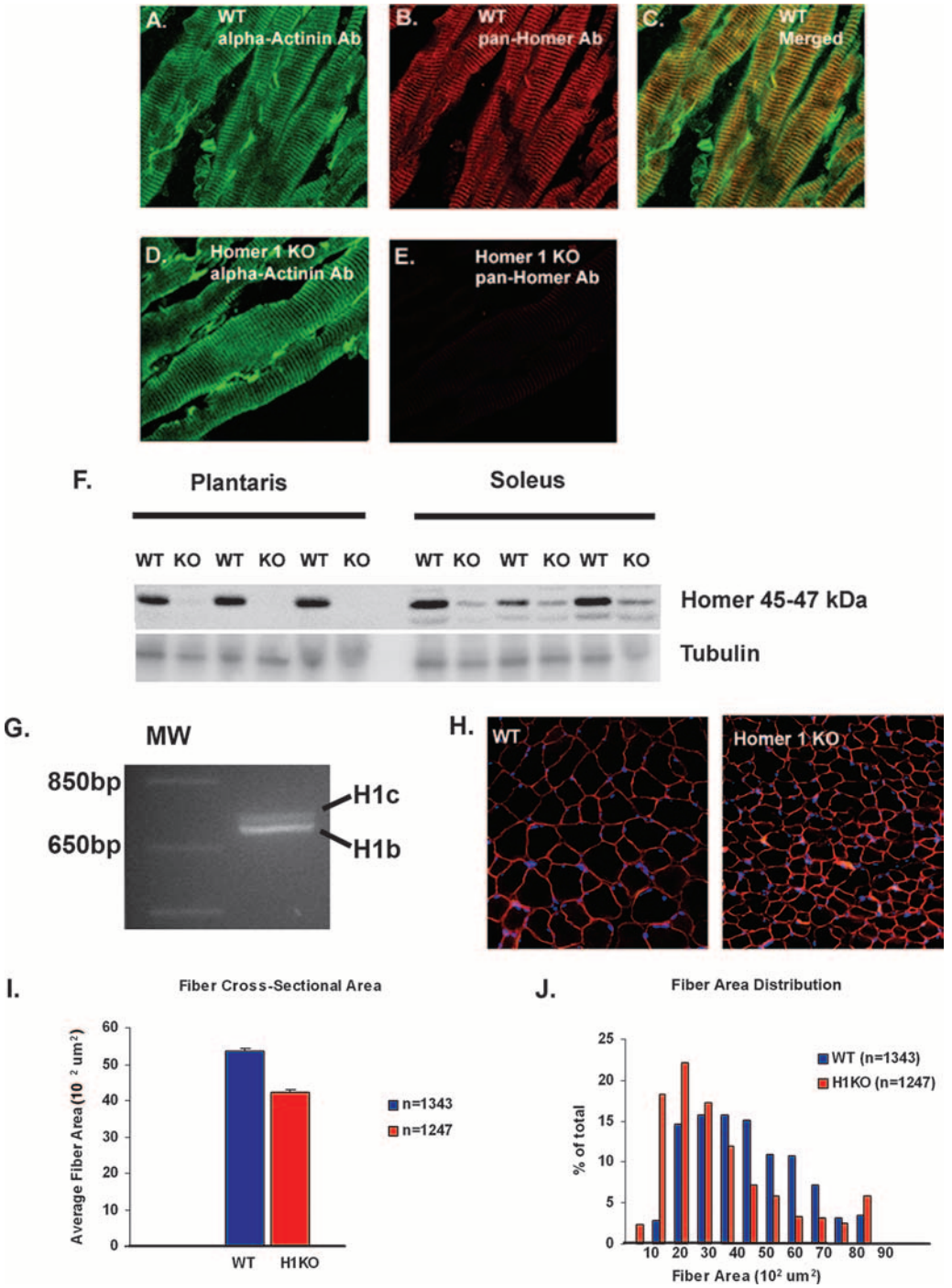

FIG. 1. Homer 1 colocalizes with alpha-actinin at the Z-disk. (A) Immunostaining of alpha-actinin in adult WT plantaris muscle. (B) Immunostaining of adult WT plantaris muscle using a pan-Homer Ab. (C) Merged image of panels A and B shows that Homer proteins and alpha-actinin colocalize. (D) Immunostaining of alpha-actinin in Homer 1 KO skeletal muscle. (E) Immunostaining of Homer 1 KO skeletal muscle using a pan-Homer Ab. (F) Western blotting using a pan-Homer Ab shows Homer expression in predominantly fast-twitch (plantaris) and predominantly slow-twitch (soleus) skeletal muscles from WT and Homer 1 KO mice. Non-Homer 1 isoforms are expressed in soleus muscle. (G) RT-PCR of cDNA generated from plantaris muscle shows the expression of coiled-coil Homer 1 isoforms, Homer 1b and Homer 1c, in adult mouse skeletal muscle. (H) DAPI (4′,6′-diamidino-2-phenylindole [blue]) and dystrophin (red) immunostaining of WT and Homer 1 KO mouse muscle. (I) Cross-sectional area of myofibers from muscles of Homer 1 KO (H1KO) mice ($n = 1247$) compared with WT littermates ($n = 1343$). Fiber cross-sectional area was $42.1 \times 10^2 \pm 80\ \mu m^2$ in Homer 1 KO mice versus $53.6 \times 10^2 \pm 65\ \mu m^2$ in WT littermate controls (mean ± SE; $P < 0.05$). (J) Distribution of muscle fiber cross-sectional areas from WT (blue) and Homer 1 KO mice (red).

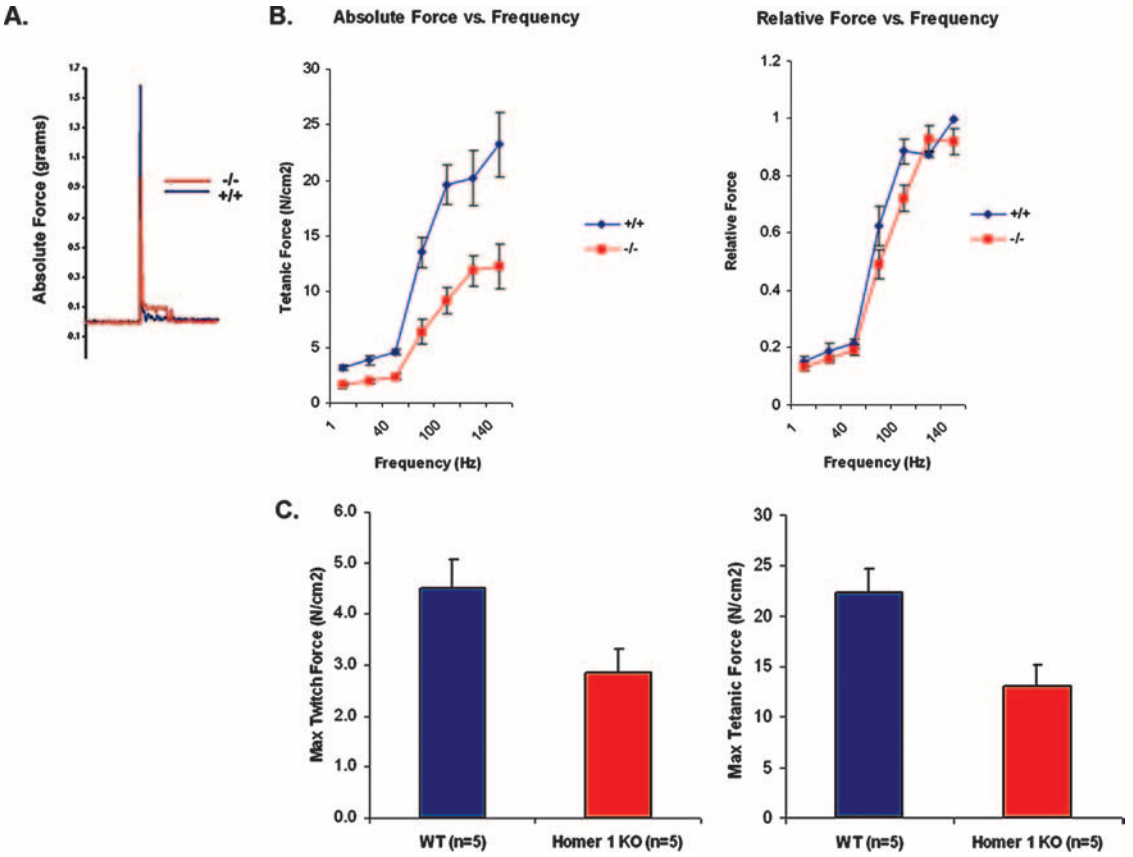

FIG. 2. Loss of Homer 1 results in decreased skeletal muscle contractility. (A) Representative tracings of twitch force generated by WT (blue) and Homer 1 KO (red) skeletal muscle display a delayed relaxation phase and a marked reduction in twitch force in Homer 1 KO muscle. (B) Force production was reduced over a range of stimulation frequencies (1 to 140 Hz), indicating a primary defect in contractility ($n = 5$, WT and KO). No significant difference was observed in the frequency at which maximum force was obtained (i.e., shift in the relative force-frequency curve) to suggest a defect in EC coupling in Homer 1 KO mice. (C) Homer 1 KO muscle exhibits significant decreases in both maximum twitch and tetanic force ($P < 0.05$). Force measurements shown are normalized to muscle cross-sectional area.

tial or L-type current between Homer 1 KO myotubes and control myotubes from WT littermates (not shown). As Homer proteins have been reported to interact with multiple TRP channels, we hypothesized that loss of Homer 1 would result in alterations in the electrophysiological properties of myotubes consistent with increased TRP channel activity. We then designed whole-cell patch-clamp experiments to test this hypothesis. With a holding potential of −60 mV and an inverted ramp protocol from +100 to −100 mV, we recorded an increase in outwardly rectifying current in Homer 1 KO myotubes compared to control myotubes isolated from WT littermates (Fig. 3A and B). Treatment with GsMTx4 peptide, a component of tarantula toxin and an inhibitor of stretch-activated channels (42), blocked the increased current seen in Homer 1 KO myotubes (Fig. 3C and D). Thus, our data confirm that the increased current seen in Homer 1 KO myotubes is due to dysregulation of mechanosensitive channels. The increased outwardly rectifying current strongly suggested a TRP current as the pipette and bath solution were configured to minimize voltage-gated calcium, sodium and potassium currents (see Materials and Methods).

The effect of loss of Homer on calcium signaling. As stated previously, measurements of the relative force-frequency relationship in Homer 1 KO mice and controls did not suggest a defect in EC coupling. In addition, we observed no differences in the amount of ryanodine receptor expression on a protein level or in the Ca^{2+} dependence of [^{3}H]ryanodine binding as a measurement of receptor activity in isolated microsomes between Homer 1 KO mice and WT controls (not shown). Thus, although reports have suggested that Homer proteins regulate that gating of the ryanodine receptor, we saw no obvious defects in EC coupling in the Homer 1 KO mice (11, 19, 38, 39).

Measurements of calcium transients showed no difference in the response to stimulation with KCl (30 mM) or carbachol (100 μM). We also observed no difference in calcium influx after store depletion in Homer 1 KO myotubes compared to WT controls (data not shown). However, at early time points of myotube development, markedly abnormal calcium transients were seen in Homer KO myotubes stimulated with caffeine (15 mM). The disorganized calcium transients induced by caffeine were dependent on the presence of extracellular calcium, implicating disordered calcium entry into myotubes as opposed to a defect in the release of internal stores (see Videos S1 and S2 in the supplemental material). Consistent with this observation, we did see a significant increase in spontaneous barium influx, a surrogate measure of calcium influx, in

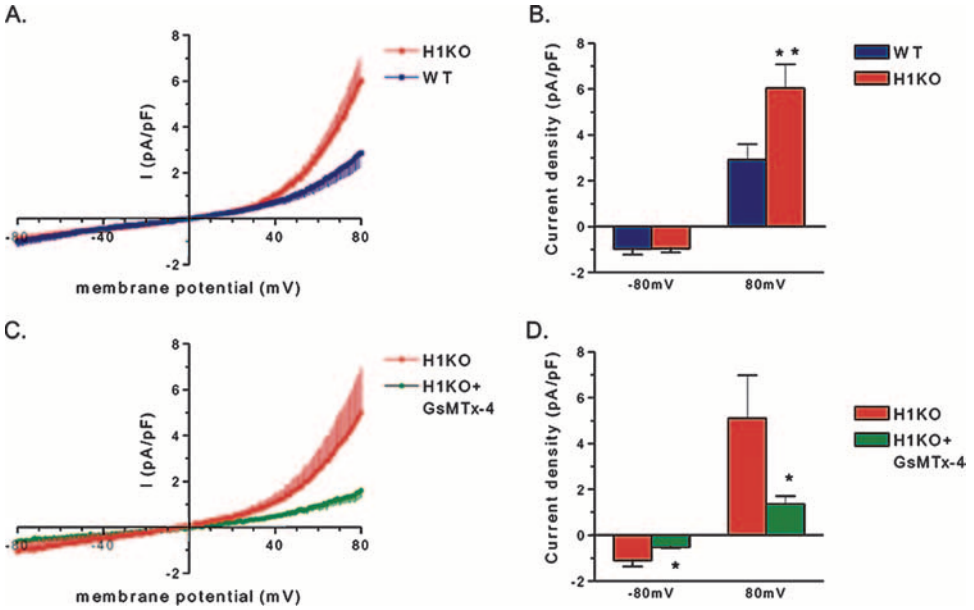

FIG. 3. Membrane current of Homer 1 knockout (H1KO) versus WT day 5 myotubes. (A) Current density-voltage (*I-V*) relationships of whole-cell current of Homer 1 KO (H1KO; red) versus WT (blue) myotubes. Currents were induced by 200-ms voltage ramp protocols (1 mV/ms, from 100 mV to −100 mV) with a holding potential of −60 mV. Currents were normalized to membrane capacitance and shown in averaged traces. Vertical bars represent the standard error of the mean. (B) Group mean current amplitudes of WT (blue; $n = 9$) versus H1KO (red; $n = 11$) at −80 mV (downward) and +80 mV (upward) (**, $P < 0.01$). (C) Effect of tarantula toxin (5 μM GsMTx-4) on membrane current of KO myotubes. GsMTx-4 (green) inhibited membrane current at both positive and negative membrane potentials. (D) Group mean values of Homer 1 KO control (red) versus GsMTx-4 (green) at −80 mV (downward) and +80 mV (upward) (*, $P < 0.05$, $n = 5$).

Homer 1 KO myotubes that was absent in WT controls (Fig. 4A). Rates of spontaneous barium influx were measured in the presence of verapamil, an L-type calcium channel blocker, excluding the possibility that this cation influx occurred through voltage-gated calcium channels.

To determine if the spontaneous cation influx we observed in KO myotubes was directly related to loss of coiled-coil Homer 1 isoforms, KO myotubes were transfected with either the coiled-coil isoform, Homer 1b, or Homer 1a, which lacks the coiled-coil domain and is unable to form multimers. Transient reexpression of Homer 1b but not Homer 1a rescued the phenotype in Homer 1 KO myotubes. Expression of Homer 1b in the Homer 1 KO background ($n = 44$) significantly blocked the spontaneous cation influx that was observed in KO myotubes ($n = 10$), whereas expression of Homer 1a had no significant effect ($n = 46$) (Fig. 4B). The average slope of spontaneous cation influx was $(1.21 \pm 0.02) \times 10^{-2}$ arbitrary units/s in Homer 1 KO myotubes transfected with control vector versus $(1.01 \pm 0.01) \times 10^{-2}$ arbitrary units/s in Homer 1 KO myotubes transfected with Homer 1b ($P < 0.001$). These findings suggested that self-multimerization of Homer 1 proteins through their coiled-coil domains was important for regulation of calcium influx.

Given the alterations in current density we observed in the experiment shown in Fig. 3, we felt that the spontaneous cation influx we observed in Homer 1 KO myotubes was likely due to dysregulation of a mechanosensitive TRP channel. We performed gene silencing of TRPC1 to test this hypothesis. Homer 1 KO myotubes were transfected with either a control short hairpin RNA (shRNA) construct ($n = 22$), a shRNA construct for silencing of TRPC1 (SIL A, $n = 24$; SIL B, $n = 28$), or a noneffective shRNA construct designed against TRPC1 (SIL C; $n = 40$). Homer 1 KO myotubes transfected with either one of the two shRNA constructs for silencing of TRPC1 (SIL A or SIL B) showed significant inhibition of spontaneous cation influx, closely approximating the response of WT myotubes. The average slope of spontaneous cation influx was $(1.33 \pm 0.07) \times 10^{-2}$ arbitrary units/s in Homer 1 KO myotubes transfected with control shRNA vector versus $(1.01 \pm 0.002) \times 10^{-2}$ in Homer 1 KO myotubes transfected with SIL A and $1.03 \pm 0.004 \times 10^{-2}$ in Homer 1 KO myotubes transfected with SIL B ($P < 0.001$ for SIL A and SIL B versus control). Both of two control (scrambled) shRNA constructs had no effect on the spontaneous cation influx observed in Homer 1 KO myotubes. Additionally, a noneffective silencing construct designed against TRPC1 had no effect on spontaneous cation influx in Homer 1 KO myotubes and served as an important additional control (SIL C). Knockdown of TRPC1 expression with silencing constructs (SIL A and B) was confirmed on a protein level in myocytes after adenoviral infection (Fig. 4D).

Spontaneous calcium influx through TRP channels is likely to be responsible for the increase in basal cytosolic calcium we observed in Homer 1 KO myotubes compared to controls (287 nM versus 118 nM, $P < 0.05$) (Fig. 4E). Interestingly a similar abnormality in calcium influx through TRP channels and increase in basal cytosolic calcium have been described in *mdx* myotubes lacking dystrophin (17). Integrity of the Z-disk/costamere complex is a key determinant of the mechanical properties of the developing myotube. Previous work has shown that myotube stiffness is dependent on the integrity of cytoskeletal proteins that are targets of calpains, calcium-dependent

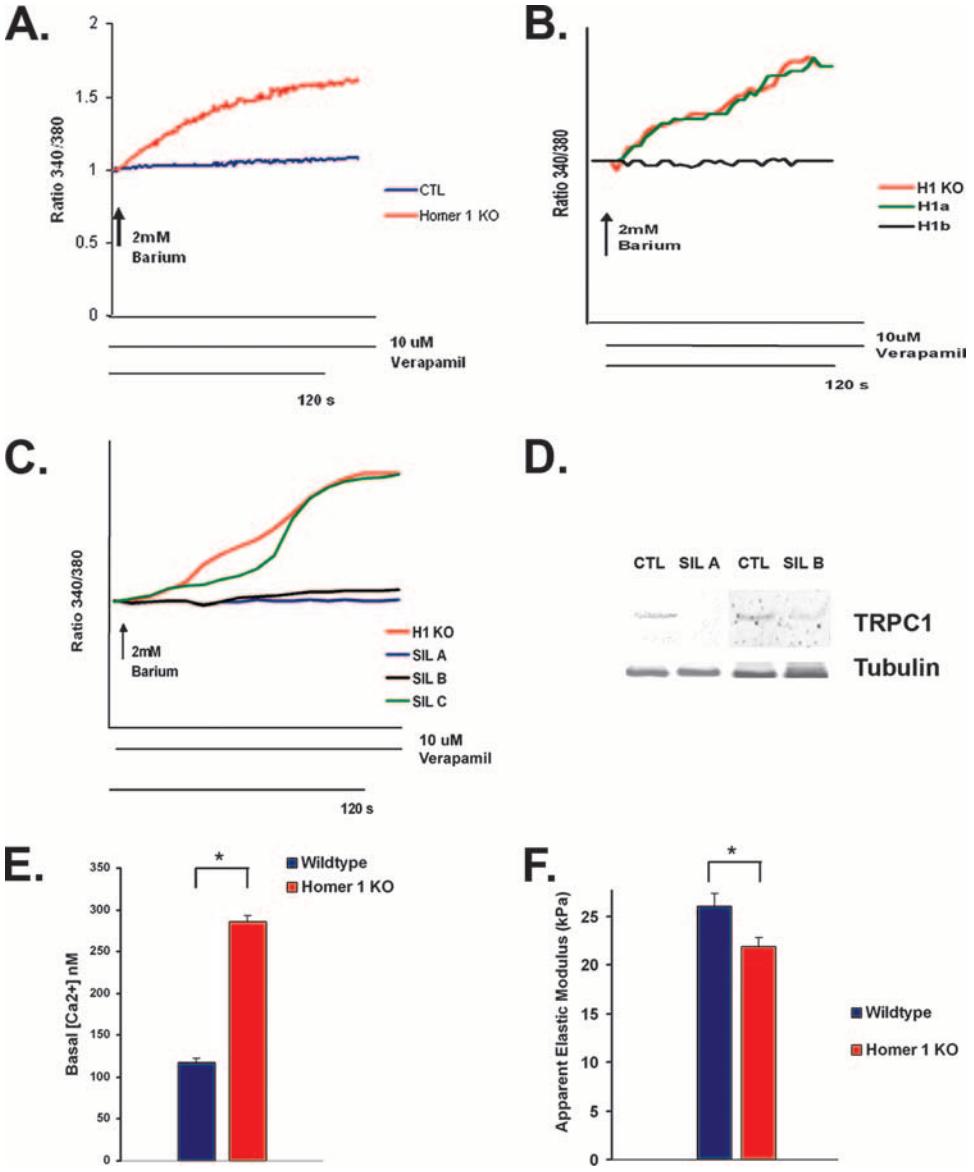

FIG. 4. Homer 1 KO myotubes exhibit abnormal TRP channel activation. (A) Homer 1 KO and WT myotubes were placed in a zero calcium solution in the presence of verapamil, followed by the readdition of 2 mM barium. Spontaneous barium influx was seen in Homer 1 KO myotubes (red) but not in controls (blue). (B) Homer 1 KO myotubes were transfected with empty vector expressing YFP alone (H1KO; $n = 10$) or along with an expression vector for either Homer 1a (H1a; $n = 46$) or Homer 1b (H1b; $n = 44$). Reexpression of Homer 1b (black trace) significantly inhibited the spontaneous cation influx observed in Homer 1 KO myotubes, while reexpression of Homer 1a (green trace) had no effect. (C) Homer 1 KO myotubes were transfected with either a control shRNA construct (H1KO; $n = 22$), an shRNA construct for silencing of TRPC1 (SIL A [$n = 24$] or SIL B [$n = 28$]), or a noneffective shRNA construct designed against TRPC1 (SIL C; $n = 40$). Silencing of TRPC1 (blue trace, SIL A; black trace, SIL B) significantly inhibited the spontaneous cation influx observed in Homer 1 KO myotubes. Marked spontaneous cation influx was still observed in Homer 1 KO myotubes transfected with a control shRNA construct (red trace) or a noneffective TRPC1 shRNA construct (green trace). (D) Knockdown of TRPC1 expression in myocytes with silencing constructs (SIL A and SIL B) was confirmed on a protein level by Western blotting after adenoviral infection. (E) Bar graph showing increased basal cytosolic calcium concentration in Homer 1 KO myotubes ($n = 28$) compared with controls ($n = 16$). (F) Primary skeletal myocytes were isolated from Homer 1 KO neonates and their WT littermate controls and allowed to differentiate into myotubes. After 5 days of differentiation, myotube stiffness was measured using AFM ($n = 25$ for WT and KO). Homer 1 KO myotubes exhibited a significant decrease in stiffness as expressed by the apparent elastic modulus. CTL, control.

proteases (33, 44). In these previous reports, increased calpain activity was associated with deceased myotube stiffness as measured by the transverse apparent elastic modulus. Because we observed that Homer 1 KO mice showed evidence of abnormal calcium influx, which would be expected to result in increased calpain activity, we hypothesized that loss of Homer would lead to alterations of the mechanical properties of myotubes. We isolated primary myotubes from Homer 1 KO mice and their WT littermates and allowed them to differentiate into myotubes for 5 days in low-serum differentiation medium; we then measured membrane stiffness using AFM. Homer 1 KO myotubes had a significant decrease in membrane stiffness, as

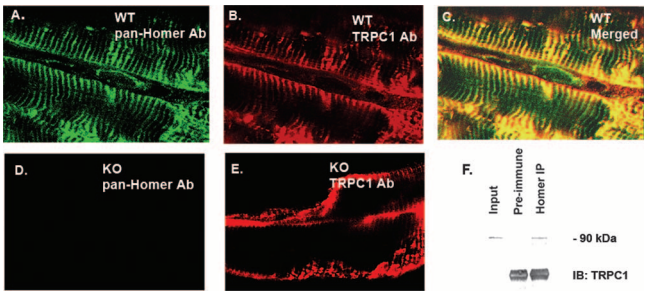

FIG. 5. Partial colocalization and coimmunoprecipitation of Homer and TRPC1 in adult skeletal muscle. (A) Immunostaining of adult WT plantaris muscle using a pan-Homer Ab. (B) Immunostaining of adult WT plantaris muscle for TRPC1. (C) Merged image of panels A and B shows that Homer 1 proteins and TRPC1 show significant colocalization at the costamere. (D) Immunostaining of Homer 1 KO plantaris muscle using a pan-Homer Ab. (E) Immunostaining of Homer 1 KO skeletal muscle using a TRPC1 Ab. (F) Coimmunoprecipitation of Homer and TRPC1 from a mouse gastrocnemius muscle protein lysate. Preimmune rat serum was used as a negative control. A pan-Homer Ab was used for immunoprecipitation (IP) of endogenous Homer protein, followed by SDS-PAGE and immunoblotting (IB) for TRPC1.

exhibited by a decrease in their apparent elastic modulus, compared to WT myotubes (Fig. 4F) ($P < 0.05$). This decrease in membrane stiffness is consistent with a defect in the integrity of the Z-disk/costamere complex due to increased TRP current and excessive calpain activity.

Homer 1 and TRPC1 localization in skeletal muscle. A direct interaction between Homer 1 and TRPC1 has been previously described and is dependent on the N-terminal EVH1 domain of Homer 1 isoforms and interaction sites on both the N and C termini of TRPC1 (43), but this interaction has not been confirmed in skeletal muscle. Because our results showed a functional interaction (Fig. 4), we investigated the spatial expression patterns of Homer 1 proteins and TRPC1 in skeletal muscle. Immunostaining for Homer 1 isoforms in adult skeletal muscle revealed Homer 1 expression along the entire length of the Z-disk/costamere while TRPC1 expression was localized to the costamere and sarcolemma (Fig. 5A to E). Although Homer and TRPC1 showed distinct spatial expression patterns, there was significant colocalization at the costamere (Fig. 5C). Importantly, we observed no significant difference in the spatial expression pattern of TRPC1 in Homer 1 KO adult skeletal muscle compared with adult WT skeletal muscle (Fig. 5B and E). We also observed no difference in the surface expression of TRPC1 protein in cultured myotubes derived from Homer 1 KO mice compared with those from WT mice, either by immunostaining or by surface biotinylation (data not shown). We then performed a coimmunoprecipitation assay which confirmed an interaction between endogenous Homer and TRPC1 protein in adult skeletal muscle (Fig. 5F).

Homer expression in mouse models of muscular dystrophy. Abnormal calcium influx through TRP channels has been described in skeletal muscle from patients with Duchenne's muscular dystrophy (DMD) and in *mdx* mice lacking dystrophin, although the mechanism of TRP channel dysregulation in this disease is uncertain (16, 37). We measured Homer protein expression in tibialis anterior muscle from *mdx* mice as well as in *mdx* and utrophin double KO mice (*mdx*/*utr*$^{-/-}$) which lack both dystrophin and utrophin and have a more severe myopathic phenotype resembling DMD. We saw a significant decrease in Homer expression in muscles taken from both *mdx*$^{-/-}$ and *mdx*/*utr*$^{-/-}$ mice, suggesting that loss of Homer may contribute to the abnormal calcium influx through TRP channels seen in DMD (Fig. 6C and D).

The calcium overload which results from abnormal TRP channel activity is felt to contribute to the myopathic process in

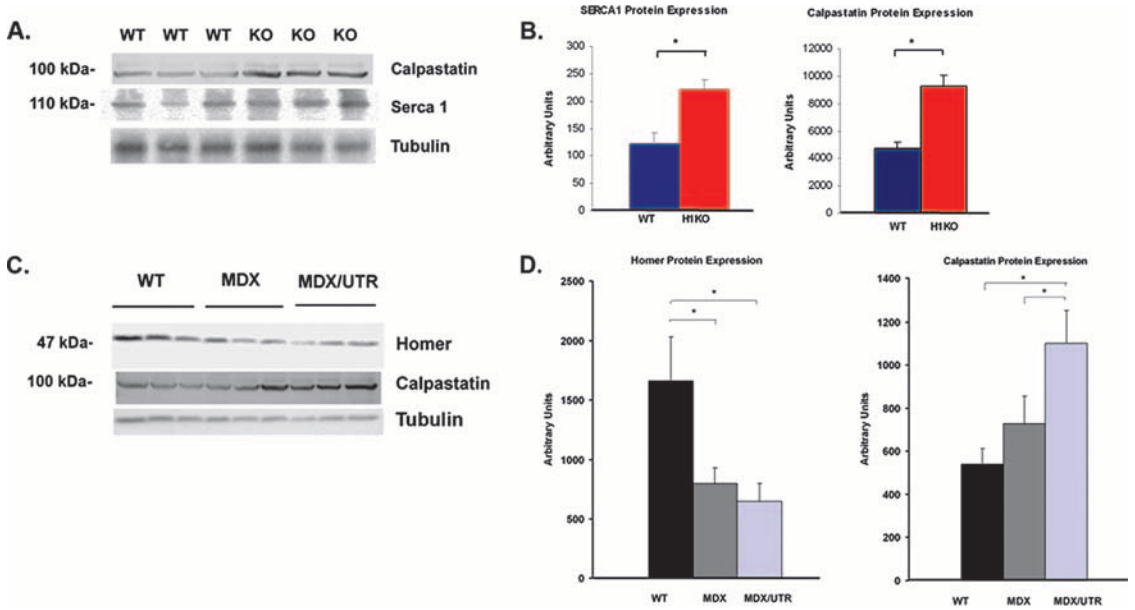

FIG. 6. (A) Western blotting showing expression of calpastatin and SERCA1 in WT and Homer 1 KO gastrocnemius muscle. (B) Bar graphs summarizing expression data from Western blots in arbitrary units. (C) Western blots showing Homer protein and calpastatin expression in WT, MDX$^{-/-}$, and MDX/UTR$^{-/-}$ double KO mice. (D) Bar graphs summarizing expression data from the above Western blots in arbitrary units.

DMD through the activation of calpains, a family of calcium-activated proteases, resulting in excessive muscle protein degradation (29, 30). Calpastatins are a family of endogenous calpain inhibitors that are upregulated in response to the stress of excessive calpain activity as part of a compensatory response (30). We show an inverse relationship between Homer expression and calpain activation. While Homer expression is downregulated in *mdx*$^{-/-}$ and *mdx*/*utr*$^{-/-}$ models of muscular dystrophy, we see a concomitant increase in calpastatin expression, consistent with the increase in calpain activation described in these models (Fig. 6C and D). Furthermore, we see the same evidence of increased calpain activation in the Homer 1 KO mice. Homer 1 KO mice exhibited a significant increase in calpastatin expression, closely mimicking the expression pattern seen in mouse models of muscular dystrophy (Fig. 6A and B). We also observed an increase in expression of SERCA1, consistent with a compensatory response to increased cytosolic calcium. Therefore, we conclude that abnormal influx of calcium through TRP channels contributes to the myopathy observed in the Homer 1 KO mice.

DISCUSSION

The principle finding of this study identifies Homer 1 as a regulator of mechanosensitive TRP channels in skeletal muscle. Skeletal muscle from mice lacking Homer 1 displays a reduction in force generation over a range of stimulation frequencies, reflecting increased muscle damage independent of a defect in either motor nerve innervation or EC coupling. Myotubes from Homer 1 KO cells display increased TRP channel current and spontaneous calcium influx that results in a myopathy. Thus, these studies provide direct evidence that Homer 1 defines a scaffolding protein within myotubes that is essential for regulation of TRPC1, which has previously been shown to be activated by mechanical stretch (24). In our model (Fig. 7), coiled-coil Homer proteins (i.e., Homer 1b and 1c) link TRPC1 channels to the Z-disk/costamere, where they are poised to respond to stretch. In response to stretch, these mechanosensitive TRP channels are activated, but in the absence of Homer, dysregulation of TRPC1 channels results in spontaneous calcium influx, activation of calcium-dependent proteolysis via calpains, and degradation of cytoskeletal elements resulting in a myopathy. Homer proteins have also been shown to interact with the actin cytoskeleton which, in turn, has been shown to regulate TRPC1 function (21, 36). As TRPC channels have been noted to form heteromers, we cannot rule out the possibility that other TRPC channels may be involved in this process, but gene silencing of TRPC1 resulted in nearly complete inhibition of the spontaneous cation influx noted in Homer 1 KO myotubes. While Homer 1 isoforms represent the predominant isoforms of both fast- and slow-twitch muscle, slow-twitch muscle expresses both Homer 1 and 2 isoforms (Fig. 1F). We would therefore expect the dysregulation of TRPC1 to be fiber type dependent.

We had previously observed that Homer is expressed as part of the myogenic differentiation program and that overexpression of Homer 2b resulted in enhanced myotube differentiation through its effects on calcineurin/NFAT activation (31). Impaired myogenic differentiation of Homer 1 KO myotubes may have been expected based on these results. However, Homer 1 KO skeletal myocytes showed normal myotube formation and no difference in the expression of myoglobin compared with WT myotubes, the expression of which is dependent on calcineurin/NFAT signaling (data not shown). The Homer 1 KO mouse, therefore, appears to be a model of skeletal myopathy rather than altered calcineurin signaling.

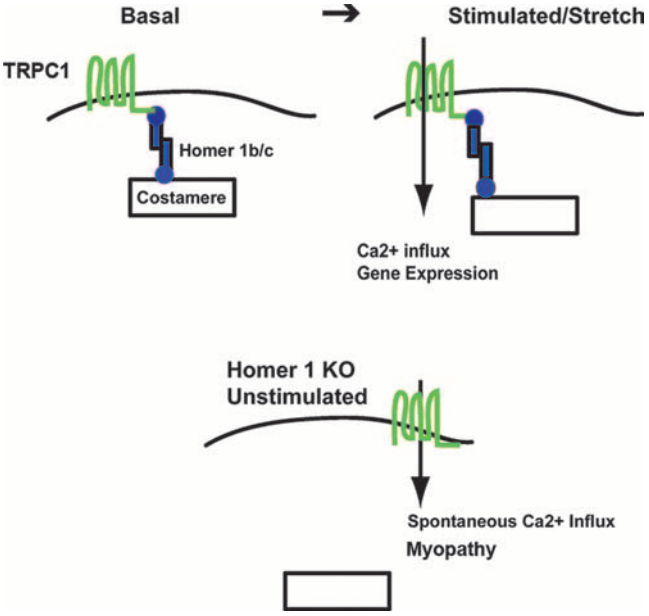

FIG. 7. Model of the role of Homer proteins in the regulation of mechanosensitive TRP channels. In the basal state, coiled-coil Homer proteins (i.e., Homer 1b and 1c) link mechanosensitive TRP channels to the Z-disk/costamere, where they are poised to respond to stretch. In response to stretch, mechanosensitive TRP channels are activated, resulting in activation of calcium-dependent signaling pathways. In the absence of Homer (bottom), dysregulation of mechanosensitive TRP channels results in spontaneous calcium influx, activation of calcium-dependent proteolysis via calpains, and degradation of cytoskeletal elements resulting in a myopathy.

These data can be reconciled with our previous work based on a model in which Homer participates in the formation of a microdomain linking TRPC1 to the costamere, the site of several signaling proteins including calcineurin. Coordinated calcium influx through TRP channels, as occurs when Homer is overexpressed, is necessary for enhanced calcineurin signaling. We have shown increased TRP channel activity in Homer 1 KO myotubes. However, increased TRP channel activity alone is not sufficient to enhance calcineurin activity when it occurs in a dysregulated manner, as in the absence of Homer 1, where we observe deleterious effects associated with spontaneous calcium influx.

The Homer 1 KO mouse represents a novel model system for studying a skeletal muscle myopathy due to the loss of a scaffolding protein which links the contractile apparatus with stretch-activated calcium signaling. This has important clinical implications for understanding mechanotransduction in skeletal and cardiac muscle. Quite recently, dysregulation of TRP channels has been associated with several human diseases and disease models (13, 25, 37, 41). The present study reveals that Homer 1 is localized to the Z-disk and that loss of Homer 1 results in a myopathy characterized by decreased contractile

force and abnormal calcium influx through mechanosensitive TRP channels. In addition to its role in anchoring actin thin filaments, the Z-disk is important for lateral force transmission as well as being the location for a variety of signaling molecules. An emerging body of evidence suggests that the Z-disk/costamere complex, with its strategic location, plays a critical role in mechanotransduction, or the conversion of mechanical forces into activation of signaling pathways. The critical function of this protein complex is further evidenced by the fact that mutations or loss of several proteins in this complex are associated with myopathies (8).

Homer expression was found to be decreased in *mdx* mice and *mdx/utr* double KO mice. Previous work has shown increased calcium influx through TRP channels in mouse models of muscular dystrophy, resulting in deleterious consequences due to calcium-dependent activation of calpains and subsequent breakdown of a variety of cytoskeletal and costameric proteins (17, 22, 29, 40). The cause of the dysregulation of TRP channels in muscular dystrophy remains unclear. One hypothesis is that calcium influx through disruptions in the sarcolemma results in activation of TRP channels. Another hypothesis supported by recent work is that the loss of the dystrophin-associated complex alters the mechanical properties of myofibers, leading to increased propensity for activation of mechanosensitive TRP channels such as TRPC1 (20, 37). The significant loss of Homer in mouse models of DMD may contribute to the TRP channel dysregulation seen in these models. Our data suggest that Homer may serve as a link between mechanical stretch and activation of mechanosensitive TRP channels. Stretch-activated channel blockade has in fact been shown to decrease the degree of membrane damage from eccentric contractions in *mdx* mouse muscle (42). Homer proteins represent an important potential target in the treatment of diseases characterized by abnormal mechanosensitive channel activation.

ACKNOWLEDGMENTS

We thank Robert Grange (Virginia Tech University) for graciously providing muscle samples from *mdx* and *mdx/utr*$^{-/-}$ mice and Shmuel Muallem (UT Southwestern) for his thoughtful review of the manuscript. We thank April Hawkins and Victoria Graham for their assistance.

Jonathan Stiber receives support from an H.H.M.I. Physician-Scientist Early Career Award, NIH/NHLBI K08 HL077520, and a Medtronic-Duke University Collaborative grant. Paul Rosenberg receives support from NIH/NHLBI K08 HL071841, a grant from the Muscular Dystrophy Association, and a grant from the Mandell Foundation.

REFERENCES

1. **Ango, F., L. Prezeau, T. Muller, J. C. Tu, B. Xiao, P. F. Worley, J. P. Pin, J. Bockaert, and L. Fagni.** 2001. Agonist-independent activation of metabotropic glutamate receptors by the intracellular protein Homer. Nature **411:** 962–965.
2. **Berthier, C., and S. Blaineau.** 1997. Supramolecular organization of the subsarcolemmal cytoskeleton of adult skeletal muscle fibers. A review. Biol. Cell **89:**413–434.
3. **Bloch, R. J., P. Reed, A. O'Neill, J. Strong, M. Williams, N. Porter, and H. Gonzalez-Serratos.** 2004. Costameres mediate force transduction in healthy skeletal muscle and are altered in muscular dystrophies. J. Muscle Res. Cell Motil. **25:**590–592.
4. **Bortoloso, E., N. Pilati, A. Megighian, E. Tibaldo, D. Sandona, and P. Volpe.** 2006. Transition of Homer isoforms during skeletal muscle regeneration. Am. J. Physiol. **290:**C711—C718.
5. **Bottai, D., J. F. Guzowski, M. K. Schwarz, S. H. Kang, B. Xiao, A. Lanahan, P. F. Worley, and P. H. Seeburg.** 2002. Synaptic activity-induced conversion of intronic to exonic sequence in Homer 1 immediate early gene expression. J. Neurosci. **22:**167–175.
6. **Collinsworth, A. M., S. Zhang, W. E. Kraus, and G. A. Truskey.** 2002. Apparent elastic modulus and hysteresis of skeletal muscle cells throughout differentiation. Am. J. Physiol. **283:**C1219–C1227.
7. **Diagana, T. T., U. Thomas, S. N. Prokopenko, B. Xiao, P. F. Worley, and J. B. Thomas.** 2002. Mutation of *Drosophila* homer disrupts control of locomotor activity and behavioral plasticity. J. Neurosci. **22:**428–436.
8. **Ervasti, J. M.** 2003. Costameres: the Achilles' heel of Herculean muscle. J. Biol. Chem. **278:**13591–13594.
9. **Eu, J. P., J. M. Hare, D. T. Hess, M. Skaf, J. Sun, I. Cardenas-Navina, Q. A. Sun, M. Dewhirst, G. Meissner, and J. S. Stamler.** 2003. Concerted regulation of skeletal muscle contractility by oxygen tension and endogenous nitric oxide. Proc. Natl. Acad. Sci. USA **100:**15229–15234.
10. **Fagni, L., P. F. Worley, and F. Ango.** 2002. Homer as both a scaffold and transduction molecule. Sci. STKE **2002:**RE8. doi: 10.1126/stke.2002.137.re8.
11. **Feng, W., J. Tu, T. Yang, P. S. Vernon, P. D. Allen, P. F. Worley, and I. N. Pessah.** 2002. Homer regulates gain of ryanodine receptor type 1 channel complex. J. Biol. Chem. **277:**44722–44730.
12. **Grynkiewicz, G., M. Poenie, and R. Y. Tsien.** 1985. A new generation of Ca2+ indicators with greatly improved fluorescence properties. J. Biol. Chem. **260:**3440–3450.
13. **Harris, P. C.** 1999. Autosomal dominant polycystic kidney disease: clues to pathogenesis. Hum. Mol. Genet. **8:**1861–1866.
14. **Hartmann, J., and A. Konnerth.** 2005. Determinants of postsynaptic Ca2+ signaling in Purkinje neurons. Cell Calcium **37:**459–466.
15. **Hayashi, M. K., H. M. Ames, and Y. Hayashi.** 2006. Tetrameric hub structure of postsynaptic scaffolding protein homer. J. Neurosci. **26:**8492–8501.
16. **Head, S. I.** 1993. Membrane potential, resting calcium and calcium transients in isolated muscle fibres from normal and dystrophic mice. J. Physiol. **469:** 11–19.
17. **Hopf, F. W., P. R. Turner, W. F. Denetclaw, Jr., P. Reddy, and R. A. Steinhardt.** 1996. A critical evaluation of resting intracellular free calcium regulation in dystrophic mdx muscle. Am. J. Physiol. **271:**C1325–C1339.
18. **Huang, G., J. Y. Kim, M. Dehoff, Y. Mizuno, K. E. Kamm, P. F. Worley, S. Muallem, and W. Zeng.** 2007. $Ca2^+$ signaling in microdomains: Homer 1 mediates the interaction between RyR2 and Cav1.2 to regulate excitation-contraction coupling. J. Biol. Chem. **282:**14283–14290.
19. **Hwang, S. Y., J. Wei, J. H. Westhoff, R. S. Duncan, F. Ozawa, P. Volpe, K. Inokuchi, and P. Koulen.** 2003. Differential functional interaction of two Vesl/Homer protein isoforms with ryanodine receptor type 1: a novel mechanism for control of intracellular calcium signaling. Cell Calcium **34:**177–184.
20. **Imbert, N., C. Vandebrouck, B. Constantin, G. Duport, C. Guillou, C. Cognard, and G. Raymond.** 1996. Hypoosmotic shocks induce elevation of resting calcium level in Duchenne muscular dystrophy myotubes contracting in vitro. Neuromuscular Disord. **6:**351–360.
21. **Itagaki, K., K. B. Kannan, B. B. Singh, and C. J. Hauser.** 2004. Cytoskeletal reorganization internalizes multiple transient receptor potential channels and blocks calcium entry into human neutrophils. J. Immunol. **172:**601–607.
22. **Iwata, Y., Y. Katanosaka, Z. Shijun, Y. Kobayashi, H. Hanada, M. Shigekawa, and S. Wakabayashi.** 2005. Protective effects of Ca2+ handling drugs against abnormal $Ca2^+$ homeostasis and cell damage in myopathic skeletal muscle cells. Biochem. Pharmacol. **70:**740–751.
23. **Kim, J. Y., W. Zeng, K. Kiselyov, J. P. Yuan, M. H. Dehoff, K. Mikoshiba, P. F. Worley, and S. Muallem.** 2006. Homer 1 mediates store- and inositol 1,4,5-trisphosphate receptor-dependent translocation and retrieval of TRPC3 to the plasma membrane. J. Biol. Chem. **281:**32540–32549.
24. **Maroto, R., A. Raso, T. G. Wood, A. Kurosky, B. Martinac, and O. P. Hamill.** 2005. TRPC1 forms the stretch-activated cation channel in vertebrate cells. Nat. Cell Biol. **7:**179–185.
25. **Reiser, J., K. R. Polu, C. C. Moller, P. Kenlan, M. M. Altintas, C. Wei, C. Faul, S. Herbert, I. Villegas, C. Avila-Casado, M. McGee, H. Sugimoto, D. Brown, R. Kalluri, P. Mundel, P. L. Smith, D. E. Clapham, and M. R. Pollak.** 2005. TRPC6 is a glomerular slit diaphragm-associated channel required for normal renal function. Nat. Genet. **37:**739–744.
26. **Salanova, M., G. Priori, V. Barone, E. Intravaia, B. Flucher, F. Ciruela, R. A. McIlhinney, J. B. Parys, K. Mikoshiba, and V. Sorrentino.** 2002. Homer proteins and InsP(3) receptors co-localise in the longitudinal sarcoplasmic reticulum of skeletal muscle fibres. Cell Calcium **32:**193–200.
27. **Sandona, D., E. Tibaldo, and P. Volpe.** 2000. Evidence for the presence of two homer 1 transcripts in skeletal and cardiac muscles. Biochem. Biophys. Res. Commun. **279:**348–353.
28. **Soloviev, M. M., F. Ciruela, W. Y. Chan, and R. A. McIlhinney.** 2000. Mouse brain and muscle tissues constitutively express high levels of Homer proteins. Eur. J. Biochem. **267:**634–639.
29. **Spencer, M. J., D. E. Croall, and J. G. Tidball.** 1995. Calpains are activated in necrotic fibers from *mdx* dystrophic mice. J. Biol. Chem. **270:**10909–10914.
30. **Spencer, M. J., and R. L. Mellgren.** 2002. Overexpression of a calpastatin transgene in *mdx* muscle reduces dystrophic pathology. Hum. Mol. Genet. **11:**2645–2655.
31. **Stiber, J. A., N. Tabatabaei, A. F. Hawkins, T. Hawke, P. F. Worley, R. S.**

Williams, and P. Rosenberg. 2005. Homer modulates NFAT-dependent signaling during muscle differentiation. Dev. Biol. **287:**213–224.

32. **Szumlinski, K. K., K. D. Lominac, M. J. Kleschen, E. B. Oleson, M. H. Dehoff, M. K. Schwarz, P. H. Seeburg, P. F. Worley, and P. W. Kalivas.** 2005. Behavioral and neurochemical phenotyping of Homer1 mutant mice: possible relevance to schizophrenia. Genes, Brain, Behavior **4:**273–288. (Erratum, **8:**486.)
33. **Tidball, J. G.** 1991. Force transmission across muscle cell membranes. J. Biomech. **24**(Suppl. 1)**:**43–52.
34. **Tu, J. C., B. Xiao, S. Naisbitt, J. P. Yuan, R. S. Petralia, P. Brakeman, A. Doan, V. K. Aakalu, A. A. Lanahan, M. Sheng, and P. F. Worley.** 1999. Coupling of mGluR/Homer and PSD-95 complexes by the Shank family of postsynaptic density proteins. Neuron **23:**583–592.
35. **Tu, J. C., B. Xiao, J. P. Yuan, A. A. Lanahan, K. Leoffert, M. Li, D. J. Linden, and P. F. Worley.** 1998. Homer binds a novel proline-rich motif and links group 1 metabotropic glutamate receptors with IP3 receptors. Neuron **21:** 717–726.
36. **Usui, S., D. Konno, K. Hori, H. Maruoka, S. Okabe, T. Fujikado, Y. Tano, and K. Sobue.** 2003. Synaptic targeting of PSD-Zip45 (Homer 1c) and its involvement in the synaptic accumulation of F-actin. J. Biol. Chem. **278:** 10619–10628.
37. **Vandebrouck, C., D. Martin, M. Colson-Van Schoor, H. Debaix, and P. Gailly.** 2002. Involvement of TRPC in the abnormal calcium influx observed in dystrophic (*mdx*) mouse skeletal muscle fibers. J. Cell Biol. **158:**1089–1096.
38. **Ward, C. W., W. Feng, J. Tu, I. N. Pessah, P. K. Worley, and M. F. Schneider.** 2004. Homer protein increases activation of Ca2+ sparks in permeabilized skeletal muscle. J. Biol. Chem. **279:**5781–5787.
39. **Westhoff, J. H., S. Y. Hwang, R. S. Duncan, F. Ozawa, P. Volpe, K. Inokuchi, and P. Koulen.** 2003. Vesl/Homer proteins regulate ryanodine receptor type 2 function and intracellular calcium signaling. Cell Calcium **34:**261–269.
40. **Williams, I. A., and D. G. Allen.** 2007. Intracellular calcium handling in ventricular myocytes from mdx mice. Am. J. Physiol. **292:**H846—H855.
41. **Winn, M. P., P. J. Conlon, K. L. Lynn, M. K. Farrington, T. Creazzo, A. F. Hawkins, N. Daskalakis, S. Y. Kwan, S. Ebersviller, J. L. Burchette, M. A. Pericak-Vance, D. N. Howell, J. M. Vance, and P. B. Rosenberg.** 2005. A mutation in the TRPC6 cation channel causes familial focal segmental glomerulosclerosis. Science **308:**1801–1804.
42. **Yeung, E. W., N. P. Whitehead, T. M. Suchyna, P. A. Gottlieb, F. Sachs, and D. G. Allen.** 2005. Effects of stretch-activated channel blockers on $[Ca^{2+}]i$ and muscle damage in the *mdx* mouse. J. Physiol. **562:**367–380.
43. **Yuan, J. P., K. Kiselyov, D. M. Shin, J. Chen, N. Shcheynikov, S. H. Kang, M. H. Dehoff, M. K. Schwarz, P. H. Seeburg, S. Muallem, and P. F. Worley.** 2003. Homer binds TRPC family channels and is required for gating of TRPC1 by IP3 receptors. Cell **114:**777–789.
44. **Zhang, J. S., W. E. Kraus, and G. A. Truskey.** 2004. Stretch-induced nitric oxide modulates mechanical properties of skeletal muscle cells. Am. J. Physiol. **287:**C292—C299.